Biol Blood Marrow Transplant 25 (2019) 223–232

Biology of Blood and Marrow Transplantation

journal homepage: www.bbmt.org

Cellular Therapy

Manufacture of Chimeric Antigen Receptor T Cells from Mobilized Cyropreserved Peripheral Blood Stem Cell Units Depends on Monocyte Depletion

Annette Künkele[1,2,3,*], Christopher Brown[4], Adam Beebe[4], Stephanie Mgebroff[4], Adam J. Johnson[3], Agne Taraseviciute[3,5,6], Lisa S. Rolczynski[3], Cindy A. Chang[3], Olivia C. Finney[3], Julie R. Park[5,6], Michael C. Jensen[3,5,6,7]

[1] *Department of Pediatric Oncology and Hematology, Charité University Medical Center, Berlin, Germany*
[2] *Berlin Institute of Health, Berlin, Germany*
[3] *Ben Towne Center for Childhood Cancer Research, Seattle Children's Research Institute, Seattle, Washington*
[4] *Seattle Children's Research Institute, Seattle, Washington*
[5] *Fred Hutchinson Cancer Research Center, Seattle, Washington*
[6] *Seattle Children's Hospital, Department of Pediatrics, University of Washington, Seattle, Washington*
[7] *Department of Bioengineering, University of Washington, Seattle, Washington*

Article history:
Received 5 August 2018
Accepted 2 October 2018

Key Words:
Autologous cryopreserved G-CSF-mobilized PBSCs
CAR-T cell manufacturing
CD14 depletion

A B S T R A C T

Cytotoxic chemotherapy and radiation can render lymphocyte repertoires qualitatively and quantitatively defective. Thus, heavily treated patients are often poor candidates for the manufacture of autologous chimeric antigen receptor (CAR)-T cell products. In the United States and Europe, children with high-risk neuroblastoma undergo apheresis early in the course of treatment to collect peripheral blood stem cells (PBSCs) for cryopreservation in preparation for high-dose chemotherapy followed by autologous stem cell rescue. Here, we investigate whether these cryopreserved chemotherapy and granulocyte colony-stimulating factor (G-CSF)-mobilized PBSCs can serve as starting material for CAR-T cell manufacturing. We evaluated T cell precursor subsets in cryopreserved PBSC units from 8 patients with neuroblastoma using fluorescent activated cell sorting-based analysis. Every cryopreserved unit collected early in treatment contained both CD4 and CD8 precursors with significant numbers of naïve and central memory precursors. Significant numbers of $Ki67^+/PD1^+$ T cells were detected, presumably the result of chemotherapy-induced lymphopenia and subsequent homeostatic proliferation. Cryopreserved PBSC units containing 56 to 112 $\times$ 10^6 T cells were amenable to immunomagnetic selection, CD3 $\times$ 28 bead activation, lentiviral transduction, and cytokine-driven expansion, provided that CD14 monocytes were depleted before the initiation of cultures. Second- and third-generation CD171 CAR^+ CD4 and CD8 effector cells derived from cryopreserved units displayed antineuroblastoma lytic potency and cytokine secretion comparable to those derived from a healthy donor and mediated in vivo antitumor regression in NSG mice. We conclude that cryopreserved PBSCs procured via standard methods during early treatment can serve as an alternative starting source for CAR-T cell manufacturing, extending the options for heavily treated patients.

INTRODUCTION

The robust clinical activity of CD19-specific chimeric antigen receptor (CAR)-T cell immunotherapy in the treatment of B cell malignancies has generated interest in developing similar strategies for solid tumor immunotherapy. Neuroblastoma, the most common extracranial malignant solid tumor in children, arises from the sympathoadrenal lineage of the neural crest [1]. Treatment protocols for high-risk neuroblastoma in the United States and Europe currently include the harvest of granulocyte colony-stimulating factor (G-CSF)-mobilized apheresis products, which are intended for autologous rescue following myeloablative therapy [2,3]. Although polychemotherapy, autologous stem cell transplantation, anti-GD2 monoclonal antibody, and retinoic acid regimens induce initial remission in most patients, high-risk neuroblastoma frequently relapses as a highly resistant disease, demonstrating the urgent need for additional consolidative modalities, such as CAR-T cell immunotherapy [4].

We previously defined CD171 (also known as L1CAM) as a target antigen for CAR-T cell therapy in pediatric neuroblastoma

Financial disclosure: See Acknowledgments on page 231.

* Correspondence and reprint requests: Annette Künkele, MD, Department of Pediatric Hematology and Oncology, Charité–Universitätsmedizin Berlin, Augustenburger Platz 1, 13353 Berlin, Germany.
E-mail address: Annette.kuenkele@charite.de (A. Künkele).

https://doi.org/10.1016/j.bbmt.2018.10.004
1083-8791/

and have defined second- and third-generation CAR constructs that selectively target a subset of CD171 molecules enriched on tumor cells based on aberrant glycosylation [5,6]. CD171 is a homotypic adhesion molecule that contributes to the malignant biology of solid tumors and is ubiquitously expressed in a homogeneous pattern by neuroblastoma at the time of diagnosis and after relapse [6–9]. A Phase I clinical trial in children with refractory or relapsed neuroblastoma has been initiated, and the tolerability of defined CD4/CD8 T cell composition of CD171 CAR-T cell products is being studied (ClinicalTrials.gov; NCT02311621; IND FDA#16139) [6].

Pediatric patients with neuroblastoma are intensively treated with upfront cytotoxic regimens, and upon relapse frequently receive I-131 metaiodobenzylguanidine radiotherapy in addition to additional rounds of chemotherapy [10]. The T lymphocyte pool in refractory patients is damaged and depleted, making inclusion of these patients a challenge in CAR-T cell trials that perform apheresis on trial enrollment [11–13]. PBSC harvest after initial chemotherapy cycles is standard of care in many centers, and because patients typically have more PBSC units cryopreserved than are required for the consolidative autologous transplant, we sought to assess the feasibility of manufacturing CAR-T cell products from this starting material. Although the successful generation of virus-specific T cells from fresh, G-CSF-mobilized apheresis products obtained from healthy donors (HDs) has been described previously [14–16], the generation of tumor-specific CAR-T cells from cryopreserved G-CSF-mobilized apheresis products obtained from cancer patients is novel. Furthermore, the high myeloid cell content in these G-CSF-mobilized units has created the general belief that T cells derived from G-CSF-mobilized products are incapable of proliferation [17]. Here we demonstrate that PBSC products are replete with naïve and central memory precursors that, after myeloid cell depletion, are amenable to isolation, activation, transduction, and expansion into functional CAR effector cells.

MATERIALS AND METHODS

Retrospective Patient Samples

This study was conducted according to the tenets of the Declaration of Helsinki and was approved by the Institutional Review Board of Seattle Children`s Hospital (IRB #13740). The study used apheresis products from 8 patients diagnosed with neuroblastoma and treated between 2000 and 2013 at the Department of Pediatric Hematology and Oncology of Seattle Children's Hospital. All human participants provided written informed consent. Blood samples drawn from HDs served as controls.

CAR Construction and Lentiviral Production

The CD171-specific CARs used herein have been described previously [5]. In brief, the CE7 mAb scFv was codon-optimized and linked to a 12-aa ("hinge-only") spacer derived from human IgG4-Fc followed by the transmembrane domain of human CD28 and by signaling modules comprising the cytoplasmic domain of either 4-1BB alone (second-generation CAR) or CD28 (mutant) and 4-1BB (third-generation CAR). The cDNA clones encoding CAR variants were linked to a downstream T2A ribosomal skip element and truncated EGF receptor (EGFRt) and then cloned into the epHIV7 lentiviral vector [18]. The lentiviral vectors were produced at the Center for Biomedicine and Genetics at City of Hope under current good manufacturing practices (BB-MF 13830, Lentiviral Vector Manufacturing and Testing, City of Hope).

T Cell Culture

Frozen apheresis products from the patients with neuroblastomas were thawed in Normosol R plus 10% human albumin. Peripheral blood mononuclear cells (PBMCs) were isolated by standard protocol using Ficoll-Paque density gradient medium (GE Healthcare, Marlborough, MA) either from a thawed patient apheresis product or from a fresh collected HD apheresis product. Cells were then used for flow cytometry staining or, after CD14 depletion using CD14 magnetic beads (Miltenyi Biotec, Bergisch Gladbach, Germany), stimulated with anti-CD3 and anti-CD28 beads (TransAct; Miltenyi Biotec) and cultured in X-Vivo medium (Lonza, Basel, Switzerland) supplemented with 10% FBS (Atlas Biologicals, Fort Collins, CO), recombinant human IL-2 (50 U/mL), and IL-15 (.5 ng/μL). Transduction was performed 1 day after activation by centrifugation at 800 $\times$ *g* for 30 minutes at 32°C with lentiviral supernatant (multiplicity of infection, .25 to 1) supplemented with 1 mg/mL protamine sulfate (APP Pharmaceuticals, Barceloneta, Puerto Rico). Approximately 10 days later, EGFRt$^+$ T cells were enriched by immunomagnetic selection with biotin-conjugated Erbitux (Bristol-Myers Squibb, New York, NY) and streptavidin-microbeads (Miltenyi Biotec) as described previously [18]. At the end of the stimulation cycle, cells were cryopreserved in aliquots in a cell bank and thawed for subsequent in vitro and in vivo experiments.

Further expansion of CAR-T cells was carried out by coculture with irradiated PBMCs and Epstein-Barr virus-transformed lymphoblastoid cell lines with OKT3 (30 ng/mL) in Gibco RPMI medium (Thermo Fisher Scientific, Waltham, MA), supplemented with 10% FBS (HyClone; Thermo Fisher Scientific) and IL-15 (.5 ng/mL) plus IL-2 (50 U/mL) for CD8$^+$ cells and IL-15 (.5 ng/mL) plus IL-7 (5 ng/mL) for CD4$^+$ cells. In vitro experiments were performed on day 11 of expansion cultures. For in vivo experiments, cells were expanded until day 13, cryopreserved in aliquots in cell banks, and then thawed before injection.

Cell Lines

The neuroblastoma cell lines SK-N-BE(2) and SK-N-DZ were obtained from the American Type Culture Collection (Manassas, VA). The IL-2-secreting firefly luciferase (ffLuc)-expressing SK-N-DZ was generated as described previously [5]. All neuroblastoma cell lines were cultured in DMEM (Cellgro; Corning Life Sciences, Tewksbury, MA) supplemented with 10% FBS and 2 mmol/L L-glutamine.

Protein Expression

Western Blot Analysis

T cells were harvested, washed twice in PBS, and lysed in RIPA lysis buffer containing protease inhibitor (MilliporeSigma, Burlington, MA). Proteins were analyzed by SDS/PAGE followed by Western blotting using anti-CD247 (CD3-ζ; BD Biosciences, San Jose, CA), according to the manufacturer's instructions. Protein bands were detected using an Odyssey Infrared Imager (LI-COR, Lincoln, NE).

Flow Cytometry

Immunophenotyping was conducted with the following fluorophore-conjugated mAbs: CD3, CD4, CD8, CD11c, CD14, CD16, CD19, CD27, CD28, CD45RA, CD45RO, CD56, CD62L, CD69, CD123, CD127, Ki67, TIM-3, PD1 (BD Biosciences and BioLegend, San Diego, CA), and LAG3 (R&D Systems, Minneapolis, MN). Dead cells were excluded from analysis using a fixable viability stain (BD Biosciences). Cell surface expression of CD171 was analyzed using a fluorophore-conjugated mAb (clone 014; Sino Biological, Wayne, PA) or the biotinylated CE7 mAb with a fluorophore-conjugated streptavidin secondary reagent. EGFRt expression was analyzed using fluorophore-conjugated cetuximab (Bristol-Myers Squibb and BD Biosciences). Flow analyses were performed on an LSRFortessa (BD Biosciences), and data were analyzed using FlowJo software (FlowJo, Ashland, OR).

In Vitro T Cell Assays

Chromium Release Assay for Cytotoxicity

Target cells were labeled with ^{51}Cr (PerkinElmer, Waltham, MA), washed, and incubated in triplicate at 5 $\times$ 10^3 cells per well with T cells at various effector to target (E:T) ratios. Supernatants were harvested after a 4-hour incubation for γ-counting using Top Count NTX (PerkinElmer), and specific lysis was calculated as described previously [19].

Cytokine Release

A total of 5 $\times$ 10^5 T cells were plated with stimulator cells at an E:T ratio of 2:1 for 24 hours. IFNγ, TNFα, and IL-2 in the supernatant were measured using the Bio-Plex cytokine assay and Bio-Plex-200 system (Bio-Rad Laboratories, Hercules, CA).

In Vivo Experiments

NOD/SCID/γc$^{-/-}$ Mice

The NSG mouse tumor model was conducted under the Seattle Children's Research Institute's Institutional Animal Care and Use Committee-approved protocol 13853. Adult male NOD.Cg-Prkdc^{scid} Il2rg^{tm1Wjl}/SzJ (NOD scid gamma [NSG]) mice were obtained from The Jackson Laboratory (Bar Harbor, ME) or bred in-house. Mice were injected intracranially on day 0 with 2 $\times$ 10^5 IL-2-secreting, ffLuc-expressing SK-N-DZ tumor cells 2 mm lateral and .5 mm anterior to the bregma and 2.5 mm deep to the dura. Mice received a subsequent intratumoral injection of 2 $\times$ 10^6 mock-transduced or CD171 CAR-modified T cells 7 days later. For bioluminescent imaging of tumor growth, mice received i.p. injections of D-luciferin (4.29 mg/mouse; PerkinElmer). The mice were anesthetized with isoflurane and imaged using the IVIS Spectrum Imaging System (PerkinElmer) at 15 minutes after D-luciferin injection. Photon flux was analyzed within regions of interest using Living Image version 4.3 (PerkinElmer).

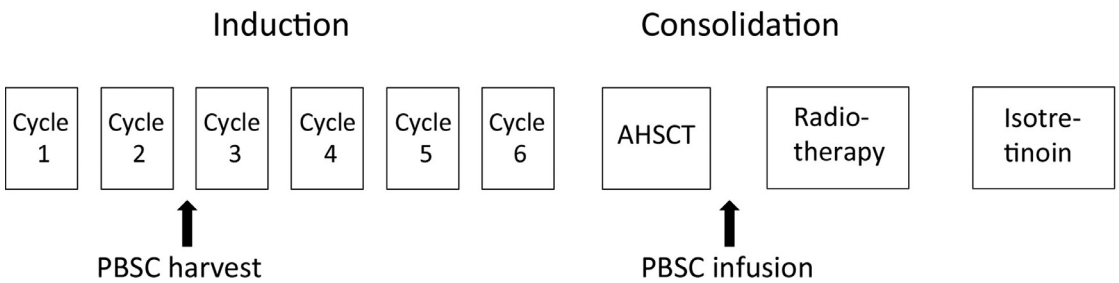

Figure 1. Treatment schema for patients with high-risk neuroblastoma responding to therapy. AHSCT, autologous hematopoietic stem cell transplantation; PBSC, peripheral blood stem cells.

Statistical Analyses

Statistical analyses were conducted using Prism (GraphPad Software, LA Jolla, CA). Data are presented as mean ± standard deviation. Means of all groups were compared for statistical differences using Student's *t* test or for statistical analyses of survival by log-rank testing. Results with a *P* value <.05 were considered significant.

RESULTS

T Cell Composition of Patient PBSC Units

The T cell populations in patient-derived cryopreserved G-CSF-mobilized PBSCs obtained early in the treatment protocol for high-risk neuroblastoma (Figure 1) were examined by multiparameter FACS analysis. We investigated cryopreserved samples from 8 patient PBSC units with high-risk neuroblastoma enrolled in Children's Oncology Group neuroblastoma trials and treated at Seattle Children's Hospital [20,21]. We analyzed mononuclear cells including T cell subsets and markers for T cell exhaustion and T cell activation status; gating strategies for FACS analysis are shown in Supplementary Figures 1 and 2. The T, B, natural killer (NK), and dendritic cell populations varied among the patients. $CD3^+$ T cells composed a mean of 23.3% (range, 12.9% to 44.3%) of mononuclear cells (Table 1), with the majority expressing the CD8 marker for T cells (mean, 63.9%; range, 34.6% to 88.7%; Figure 2A). In contrast, the majority of $CD3^+$ T cells from the 5 healthy donors expressed CD4 (mean, 64.8%; range, 60.3% to 71.4%). Frequencies of T cells displaying a central memory phenotype (T_{CM}, defined as $CD45RO^+CD62L^+$) or naïve phenotype (T_N, defined as $CD45RO^-CD62L^+$) were lower in pediatric patients than in adult HDs (patients: $CD4^+T_{CM}{}^+$: mean, 15.4%; range, 3.4% to 46.4%; $CD8^+T_{CM}{}^+$: mean, 7.9%; range, .2% to 16.0%; $CD4^+T_N{}^+$: mean, 15.6%, range, .5% to 39.8%; $CD8^+T_N{}^+$: mean, 17.4%; range, 1.4% to 44.0%). Most patient T cells were effector memory (T_{EM}, defined as $CD45RO^+CD62L^-$; $CD4^+T_{EM}{}^+$: mean, 36.3%; range, 17.7% to 67.3%; $CD8^+T_{EM}{}^+$: mean, 30.6%; range, 5.7% to 43.1%) or effector T cells (T_{Eff}, defined as $CD45RO^-CD62L^-$; $CD4^+T_{Eff}{}^+$: mean, 32.7%; range, 7.3% to 63.8%; $CD8^+T_{Eff}{}^+$: mean, 44.1%; range, 26.0% to 77.8%; Figure 2B). Patient products contained only few activated T cells (<15% $CD25^+$ or $CD69^+$); however, both CD4 and CD8 T cells in the products were proliferating ($CD4^+Ki67^+$: mean, 39.3%; range, 9.4% to 63.3%; $CD8^+Ki67^+$: mean, 53.3%; range, 5.5% to 88.2%; Figure 2C).

In contrast to HDs, high frequencies of $CD4^+$ and $CD8^+$ patient T cells expressed the inhibitory receptor programmed cell death protein 1 (PDCD1, also known as PD-1; patients: $CD4^+PD1^+$: mean, 53.3%; range, 22.7% to 97.4%; $CD8^+PD1^+$: mean, 49.6%; range, 18.5% to 74.7%; HDs: $CD4^+PD1^+$: mean, 3.0%; range, .9% to 5.7%; $CD8^+PD1^+$: mean, 3.6%; range, 1.3% to 6.2%; Figure 2D). Some patient $CD8^+$ cells also expressed hepatitis A virus cellular receptor 2 (HAVCR2, also known as TIM-3; $CD8^+TIM\text{-}3^+$: mean, 15.1%; range, 1.9% to 36.9%), consistent with previously described markers of T cells undergoing lymphopenic proliferation rather than functional exhaustion (Figure 2D) [22]. Consistent with this, T cells coexpressing LAG3, a marker of exhaustion, ($CD4^+LAG3^+$: mean, 2.3%; range, .8% to 4.7%; $CD8^+LAG3^+$: mean, .8%; range, .3% to 1.5%) were rare.

Monocyte Depletion of Thawed PBSC Units Is Required for Subsequent T Cell Activation and Proliferation

Initial attempts to thaw and expand T cells present in cryopreserved G-CSF-stimulated PBSCs failed because of the outgrowth of monocytes. Monocytes outnumbered lymphocytes by a median of >4-fold (range, 4.2- to 20.2-fold) in 6 of the 8 cryopreserved samples, whereas there were more lymphocytes than monocytes in healthy donor-derived non-G-CSF-stimulated PBSCs (Figure 3A) [23,24]. Following CD14 immunomagnetic depletion leading to a nearly 100% $CD14^-$ population, CD3 × 28 bead-activated CD4 and CD8 T cells could be expanded more than 2-fold within 9 days of culture, whereas numbers of CD3 × 28 bead-activated CD4 and CD8 T cells in nondepleted preparations decreased (Figure 3B). Therefore,

Table 1
Lineage Panel of Thawed Apheresis Products from 8 Patients with Neuroblastoma

Patient	Live Cells	Monocytes	Lymphocytes	T Cells	B Cells	NK Cells	pDCs	mDCs
1	97.3	81.6	17.7	12.9	7.85	5.75	12.7	5.02
2	99.6	31.7	63.5	31.8	7.10	3.13	2.55	2.44
3	96.1	83.5	14.3	25.3	4.38	15.5	15.8	11.7
4	97.3	89.2	10.2	15.0	1.55	5.54	20.5	27.3
5	95.7	79.0	18.9	26.6	5.59	5.58	5.02	9.92
6	85.5	94.1	4.66	13.8	1.00	22.8	10.7	29.5
7	95.0	90.9	8.76	16.6	0.56	26.0	10.2	23.2
8	98.1	27.7	71.5	44.3	3.97	1.51	1.97	1.40

pDCs indicates plasmacytoid dendritic cells; mDCs, myeloid dendritic cells .
All cells were gated on live cells. Monocytes were gated on $CD45^+CD14^+CD56^-CD3^-CD19^-CD16^-$ cells. Lymphocytes were gated on $CD45^+CD14^-$ cells. T, B, NK, and dendritic cells were gated within the lymphocytes. T cells were gated on $CD3^+$ cells; B cells, on $CD19^+$ cells. NK cells were gated on $CD3^-CD19^-CD56^+$ cells. pDCs were gated on $CD3^-CD19^-CD56^-CD16^-CD123^+$ cells. mDCs were gated on $CD3^-CD19^-CD56^-CD16^-CD11c^+$ cells.

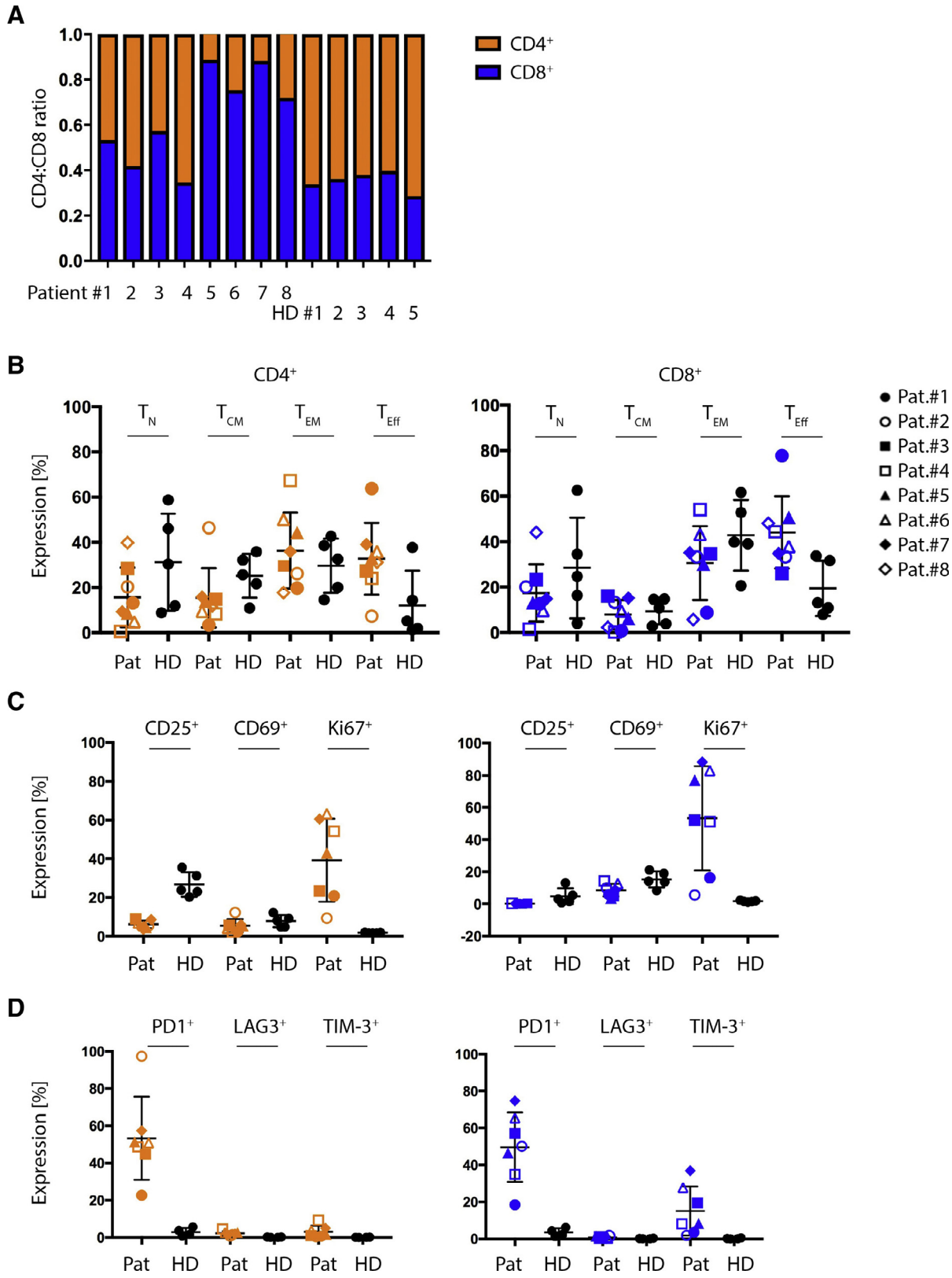

Figure 2. Phenotypic analysis of previously collected and freshly thawed apheresis products from 8 patients with neuroblastoma. (A) Flow cytometric quantification of the CD4:CD8 ratio in thawed apheresis products derived from patients and in fresh blood derived from HDs. (B) Flow cytometric quantification of CD45RO and CD62L surface expression (T_{CM}, central memory T cells: $CD45RO^+CD62L^+$; T_{EM}, effector memory T cells: $CD45RO^+CD62L^-$; T_{EFF}, effector T cells: $CD45RO^-CD62L^-$; T_N, naïve T cells: $CD45RO^-CD62L^+$). (C) Flow cytometric quantification of CD25, CD69, and Ki67 surface expression. (D) Flow cytometric quantification of PD1, LAG3, and TIM-3 surface expression. All cells were first gated on single cells, followed by live $CD3^+$ lymphocytes. Bar graphs represent mean ± SD. Pat, patient.

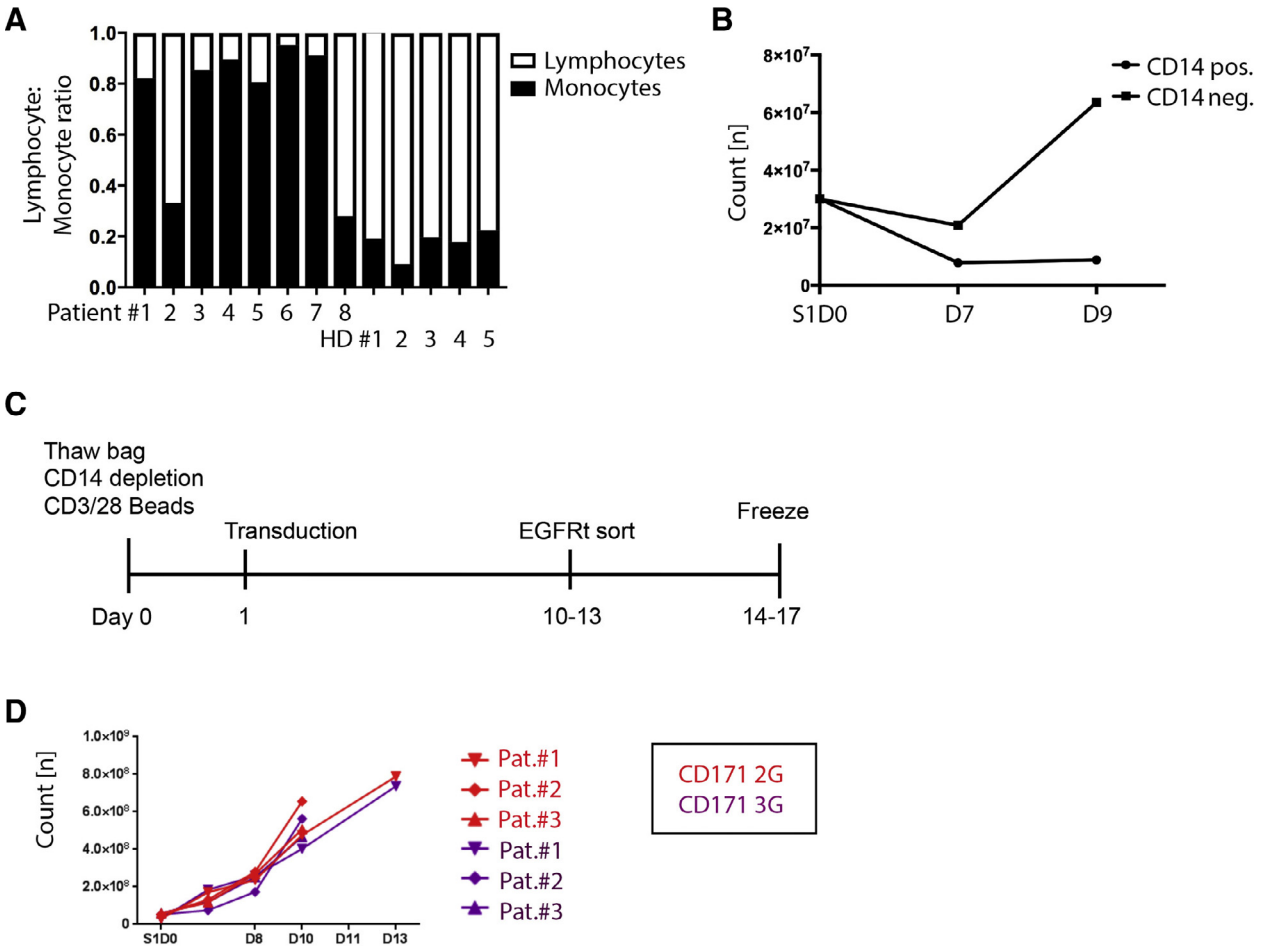

Figure 3. Manufacturing CD171 CAR-T cell products from frozen apheresis products. (A) Flow cytometric quantification of lymphocyte:monocyte ratio in thawed apheresis products derived from patients and in fresh blood derived from HDs. (B) Expansion curves of PBSCs isolated from a frozen apheresis product derived from a patient with neuroblastoma treated with and without immunomagnetic CD14 bead depletion. (C) CD171 CAR-T cell manufacturing schema. (D) Growth curves of second- and third-generation CD171 CAR-T cell products manufactured from frozen apheresis products from 3 patients with high-risk neuroblastoma. 2G, second generation; 3G, third generation.

we established a manufacturing protocol containing magnetic CD14 depletion to eliminate the growth-inhibiting monocytes before T cell activation (Figure 3C).

Mimicking the GMP manufacturing process used in the ongoing ENCIT-01 clinical trial, cells were transduced on day 1 with clinical-grade lentiviral vector containing either the second- or third-generation CD171 CAR transgene. CAR-T cell products manufactured from 3 unique G-CSF-stimulated apheresis products (collected from 3 patients with neuroblastoma) exhibited 7.9- to 26.3-fold expansion (Figure 3D) achieving T cell numbers necessary for clinical trials administering up to 1×10^7 CAR-T cells/kg body weight. The transduction efficiency for the $CD4^+$ T cells ranged from 59.6% to 74.7% for the second-generation CAR-T cell products (mean, 64.8%) and from 52.8% to 78.8% for the third-generation CAR-T cell products (mean, 66.4%). Transduction efficiency for the $CD8^+$ T cells ranged from 61.0% to 72.8% for the second-generation CAR-T cell products (mean, 65.4%) and from 71.1% to 73.0% for the third-generation CAR-T cell products (mean, 72.1%) (Figure 4A). On day 14 of ex vivo culture, CAR-T cell products displayed a viability of >80% and were enriched for homogeneous levels of EGFRt expression by cetuximab immunomagnetic positive selection [18].

Following EGFRt selection and thus enrichment of CAR-expressing T cells, the viability dropped for both second- and third-generation CAR-T cell products from patient 1, necessitating dead cell removal by Ficoll gradient centrifugation (Figure 4B). The second- and third-generation vectors performed equally well in $CD4^+$ and $CD8^+$ T cell subsets using T cell expansion, transduction efficiency and viability as endpoints. Protein expression of the CAR variants was confirmed by Western blot analysis for CD3ζ (Figure 4C). Using the same transduction and expansion strategy, we also generated control CD171 CAR-T cells obtained from a fresh HD apheresis product.

CAR-T Cells Generated from Cryopreserved Patient-Derived PBSC Products Display Anti-Tumor Activity in Vitro and in Vivo

Cryopreserved CD171 CAR-T cells were thawed and analyzed for viability using trypan blue staining. All CD171 CAR-T cell products displayed a viability >60% after thaw, meeting the current good manufacturing practices release criteria (Supplementary Figure 3A). The phenotypic classification of the final CD171 CAR-T cell products generated from cryopreserved G-CSF-stimulated PBSC apheresis products was analyzed using FACS-based analysis. The third-generation CAR-T cell products from all 3 patients contained higher numbers of $CD8^+$ T cells than the second-generation CAR-T cell products (second-generation $CD8^+$ T cells: mean, 32.2%; range, 29.0% to 36.7%; third-generation $CD8^+$ T cells: mean, 48.6%, range, 39.2% to 58.6%;

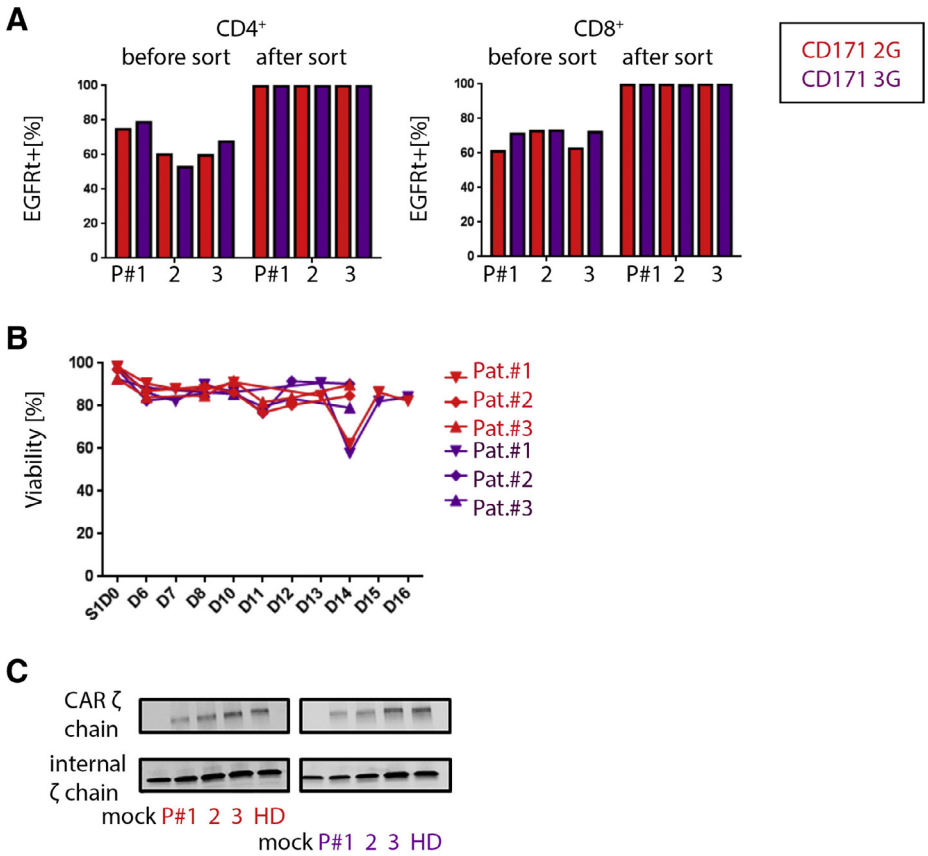

Figure 4. Enrichment for CD171 CAR-T expression. (A) EGFRt surface expression detected with cetuximab in $CD4^+$ and $CD8^+$ second- and third-generation CD171 CAR-T cell products before and after sorting for EGFRt. (B) Viability curves of second- and third-generation CD171 CAR-T cell products from 3 patients with neuroblastoma. (C) Expression levels of second- and third-generation CAR detected by Western blot analysis with an antibody against CD3ζ.

$P = .06$; Supplementary Figure 3B), but the difference did not reach statistical significance. We detected wide ranges of expression levels of CD45RO and CD62L between the manufactured products compared with the starting apheresis specimens. CD45RO and CD62L are commonly used surface markers to define T cell subsets displaying a naïve-, effector-, effector memory- or central memory-like phenotype [25]. CAR-expressing $CD4^+$ T cells displayed a 1.8-fold increase in second-generation produces and a 2-fold increase in third-generation products in $CD45RO^+CD62L^+$ cells compared with the starting material ($CD45RO^+CD62L^+$ mean in starting material, 21.5%; range, 3.4% to 46.4%; $CD45RO^+CD62L^+$ mean in manufactured second-generation product, 38.4%; range, 32.9% to 43.2%; $CD45RO^+CD62L^+$ mean in manufactured third-generation product, 42.5%; range, 27.8% to 58.3%), whereas the CAR-expressing $CD8^+$ T cells displayed a 1.3-fold increase for second generation and a .1-fold decrease for third generation in $CD45RO^+CD62L^+$ expression ($CD45RO^+CD62L^+$ mean in starting material, 10.0%; range, .8% to 16.0%; $CD45RO^+CD62L^+$ mean in manufactured second-generation product, 13.1%; range, 4.6% to 18.2%; $CD45RO^+CD62L^+$ mean in manufactured third-generation product, 8.7%; range, 4.8% to 13.4%). In general, the CAR-expressing $CD8^+$ T cells remained $CD45RO^+CD62L^-$ (second generation, 1.1-fold increase; third generation, .2-fold decrease with $CD45RO^+CD62L^-$ mean in starting material, 25.6%; range, 8.8% to 34.6%; $CD45RO^+CD62L^-$ mean in manufactured second-generation product, 26.8%; range, 12.4%-38.0%; $CD45RO^+CD62L^-$ mean in manufactured third-generation product, 20.0%; range, 11.6% to 28.3%) and $CD45RO^-CD62L^-$ (second generation, 1-fold increase; third generation, 1.1-fold increase with $CD45RO^-CD62L^-$ mean in starting material, 45.7%; range, 26.0% to 77.8%; $CD45RO^-CD62L^-$ mean in manufactured second-generation product, 44.2%; range, 28.7% to 73.9%; $CD45RO^-CD62L^-$ mean in manufactured third-generation product, 48.8%; range, 30.2% to 64.9%) following ex vivo culture (Figure 5A).

Cytolytic activity was determined in vitro using 4-hour chromium and 24-hour cytokine release assays and in vivo using a xenograft mouse model. Both second- and third-generation CAR-T cells resulted in lysis of $CD171^+$ neuroblastoma target cell lines, although greater lysis was observed following exposure to third-generation CAR-T cells (50:1 E:T ratio: median lysis of second-generation CAR-T cells, 21.8%; range, 10.3% to 32.8%; median lysis of third-generation CAR-T cells, 36.7%; range, 21.2% to 44.8%; $P < .0001$; Figure 5B). Patient-derived second- and third-generation CAR-T cells both released IFNγ (second-generation: mean, 367.8 pg/mL;, range, 268.8 to 466.3 pg/mL; third-generation: mean, 918.8 pg/mL; range, 755.7 to 1192.6 pg/mL), IL-2 (second-generation: mean, 49.7 pg/mL; range, 37.3 to 68.7 pg/mL; third-generation: mean, 66.9 pg/mL; range, 33.3 to 115.8 pg/mL) and TNFα (second-generation: mean, 658.8 pg/mL; range, 433.3 to 1024.7 pg/mL; third-generation: mean, 509.0 pg/mL; range, 173.5 to 962.5 pg/mL) during coculture with $CD171^+$ tumor cells, with a significant difference for IFNγ between second- and third-generation CAR-T cells ($P < .0001$) (Figure 5C).

To assess antitumor activity in vivo, we performed adoptive transfer experiments in NSG mice with established human neuroblastoma xenografts stereotactically implanted in the

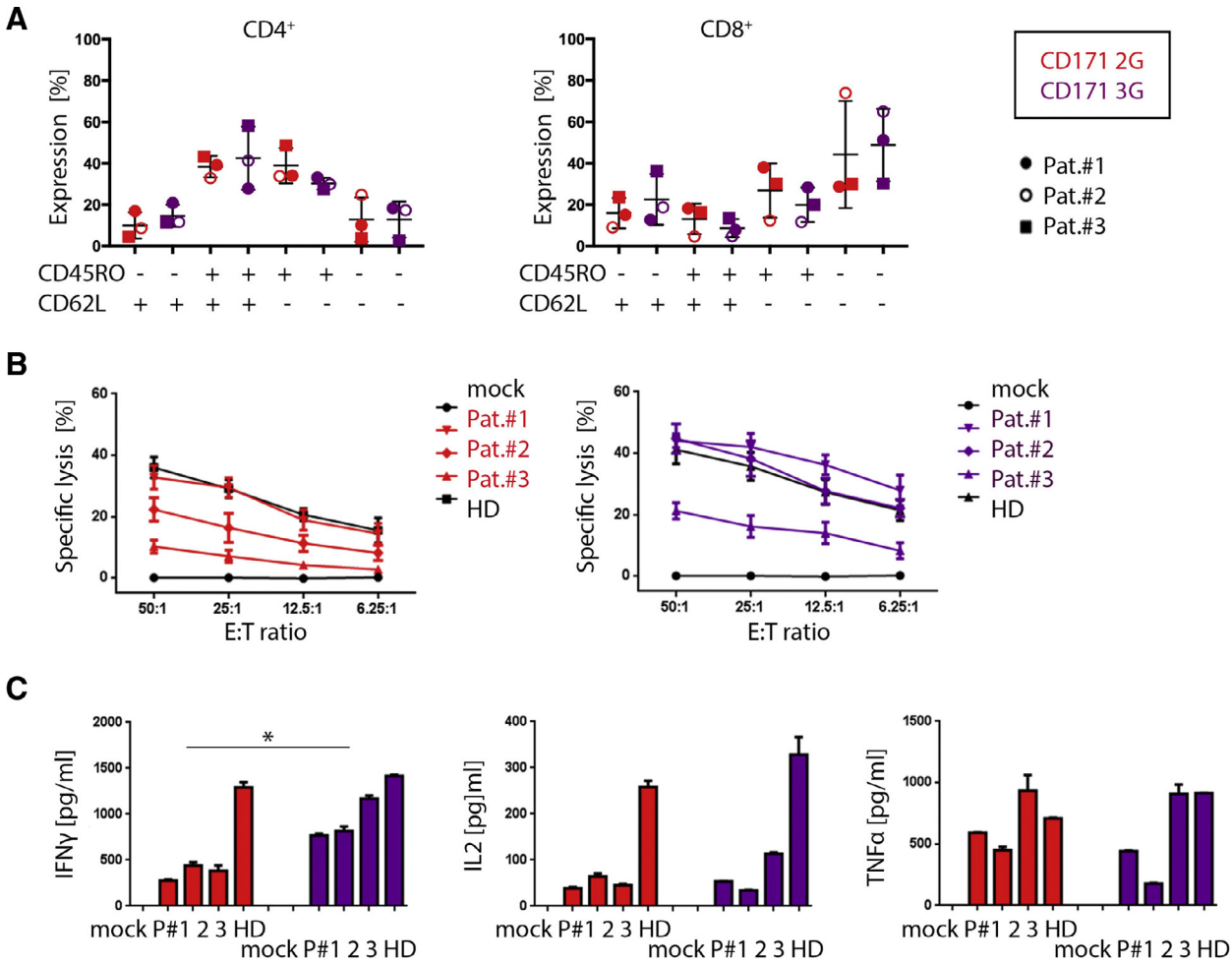

Figure 5. Phenotypic analysis and evaluation of final CAR-T cell products. (A) Flow cytometry quantification of CD45RO and CD62L expression in $CD4^+$ and $CD8^+$ second- and third- generation CD171 CAR-T cell products after thawing. Bar graphs represent the mean ± SD. (B) Antitumor lytic activity of second- and third-generation CD171 CAR CTLs determined by chromium release assay. (C) Stimulation of cytokine secretion in mixed second- and third-generation CAR-CTL tumor cultures. Error bars represent the SD of the mean of triplicates. $^*P < .05$.

cerebral hemisphere (Figure 6A). All SK-N-DZ tumor-engrafted mice treated with intratumoral injection of 2×10^6 second- or third-generation CD171 CAR-T cells generated from patient-derived G-CSF- stimulated apheresis products demonstrated tumor regression and prolonged survival compared with non-CAR-expressing negative mock control T cells (second-generation, $P < .0001$; third-generation, $P = .0001$) (Figure 6B and C).

Following cell expansion, both $CD4^+$ and $CD8^+$ CD171 CAR-T cells developed increased expression of the inhibitory receptors LAG3 and TIM-3 compared with the starting material ($CD4^+LAG3^+$ T cells: second-generation, 13.6-fold increase; mean, 18.0%; range, 15.8% to 20.0%; third-generation, 17.3-fold increase; mean, 22.9%; range, 20.5% to 26.3%; $CD8^+LAG3^+$ T cells: second-generation, 6.7-fold increase; mean, 5.3%, range, 3.0% to 7.3%; third-generation, 7.7-fold increase; mean, 6.2%; range, 5.2% to 7.3%; $CD4^+TIM\text{-}3^+$ T cells: second-generation, 94.4-fold increase; mean, 72.1%; range, 64.4% to 79%; third-generation, 93.0-fold increase; mean, 71.0%; range, 60.3% to 86.5%; $CD8^+TIM\text{-}3^+$ T cells: second-generation, 10.7-fold increase; mean, 89.0%; range, 84.2% to 92.2%, third-generation, 10.6-fold increase; mean, 87.8%; range, 84.0% to 90.1%), whereas only the $CD4^+$ cells showed increased expression of PD1 ($CD4^+PD1^+$ T cells: second-generation, 1.1-fold increase; mean, 61.8%; range, 58.4% to 67.5%; third-generation, 1.3-fold increase; mean, 73.7%; range, 71.2% to 77.0%; $CD8^+PD1^+$ T cells: second-generation, 4.6.-fold decrease; mean, 9.1%; range, 5.3% to 15.4%; third-generation, 2.7-fold decrease; mean, 15.3%; range, 8.0% to 24.4%) (Figure 6D).

Because the up-regulation of multiple inhibitory receptors did not impact the in vivo efficacy of the CD171 CAR-T cells, this up-regulation was most likely due to T cell activation and not to exhaustion [26]. This was in line with our previous finding of increasing PD1 expression on initial T cell stimulation using CD3 × 28 beads, with a return to basal levels after 6 days of expansion, underscoring its role as an early activation marker (unpublished data). Furthermore, there was a significant difference between the second- and third-generation final products only for $CD4^+PD1^+$ cells ($P = .0094$) and not for any of the other markers assessed.

DISCUSSION

CAR-T cell therapy has been the subject of a considerable number of early-phase clinical trials. Two CAR-T cell products received Food and Drug Administration approval in 2017: Kymriah (Novartis Pharmaceuticals, Basel, Switzerland) and Yescarta (Kite Pharma/Gilead Sciences, Foster City, CA). Nevertheless, manufacturing CAR-T cell products from heavily pretreated patients remains challenging, because these patients are often severely lymphopenic and have higher T_{EM} frequencies in their CD4 and CD8 T cell subsets, which are known to

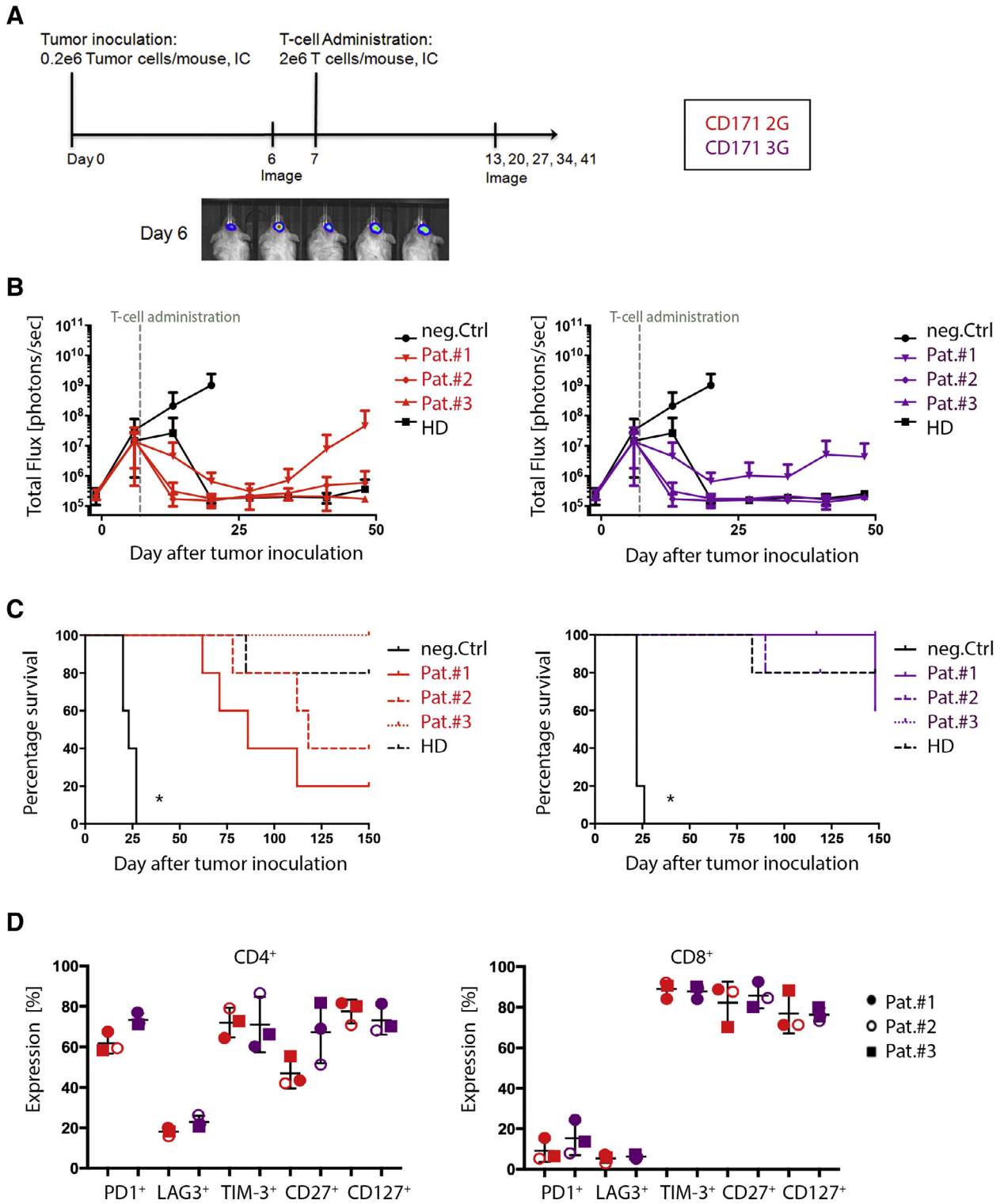

Figure 6. In vivo evaluation of CD171 CAR-T cell products. (A) Schema of the intracranial (IC) NSG mouse neuroblastoma xenograft therapy model and biophotonic signal of ffLuc$^+$ SK-N-DZ tumors on day 6 after stereotactic implantation. (B) Biophotonic tumor signal response to intratumorally injected second- and third-generation CAR CTLs (n = 5 mice per group). The mock-treated control cohort was euthanized on day 20 owing to tumor-related animal distress. (C) Kaplan-Meier survival plots of treated cohorts described in B. (D) Flow cytometry quantification of PD1, LAG3, TIM-3, CD27, and CD127 expression in CD4$^+$ and CD8$^+$ second- and third-generation CD171 CAR-T cell products after thawing. All cells were first gated on single cells and then on live CD3$^+$ lymphocytes. Bar graphs represent the mean ± SD. $^*P < .05$.

have shorter persistence and inferior antitumor immunity compared with T_{CM} subsets [27–29]. Here we provide proof of concept that bioactive CAR-T cells can be manufactured from patient-derived cryopreserved G-CSF-mobilized PBSC apheresis products.

Cryopreserved apheresis products isolated early after diagnosis have enormous potential as an alternative T cell source

to blood draws or apheresis at tumor relapse or recurrence. The use of cryopreserved PBSC products as an alternative source for generating CAR-T cells has an economic impact, avoiding not only the additional cost, but also the patient discomfort associated with an additional apheresis procedure or high-volume blood draw. Furthermore, as CAR-T cell therapy becomes a more commonly accepted first-line therapy, the current treatment protocol using intensive chemotherapy regimens administered within only a few weeks might not allow for the bone marrow recovery necessary for CAR-T cell product manufacturing, and PBSCs collected and cryopreserved early during treatment may be needed. The same applies for the administration of neuroblastoma-specific CAR-T cells in the minimal residual disease setting shortly after high-dose chemotherapy, as is currently done with NK cells. Finally, using a central specialized center or facility manufacturing CAR-T cells for different cancer entities would also become more feasible, because frozen starting products could be easily shipped to the manufacturing site for CAR-T cell production.

We have demonstrated that the use of G-CSF-stimulated cryopreserved PBSCs requires monocyte depletion before CD3 × 28 bead-based activation of isolated T cells, presumably because monocytes can phagocytose beads and potentially secrete soluble factors, such as prostaglandin E2, that inhibit T cell activation [30,31]. Monocyte-depleted PBSC product-derived T cells were amenable to lentiviral vector transduction and were competent for subsequent ex vivo proliferation to achieve the cell doses needed for CAR-T cell therapy.

We evaluated the use of cryopreserved G-CSF-stimulated PBSCs collected by apheresis very early in the treatment protocol as a source of T cells for CAR-T manufacturing. Patients with high-risk neuroblastoma were selected as an example patient cohort who could benefit from this technological advancement. For instance, patients diagnosed with primary neuroblastoma, classified as a high-risk disease, undergo dose-intensive therapy, including myeloablative consolidation chemotherapy requiring PBSC rescue. Dose-intensive chemotherapy is also often a part of treatment for relapsed or refractory neuroblastoma. We experienced difficulties expanding T cells from the 10.5% seen in the first patients with neuroblastoma enrolled in the ENCIT trial [6,13]. It is likely that the dose-intensive chemotherapy and radiotherapy to which the patients have been exposed during previous treatment has negatively impacted isolation and ex vivo expansion of isolated T cells. This is in line with results from a University of Pennsylvania study in which 24% of patients with leukemia were excluded from CD19-CAR manufacturing owing to failure in the “test expansion” performed before patient enrollment into a clinical trial [11]. The authors proposed that previous chemotherapy, especially therapy administered to patients with high-risk leukemia might have a negative impact on T cell expansion. To circumvent this problem, we propose using the cryopreserved G-CSF-stimulated PBSCs collected by apheresis early after diagnosis as a source of T cells for patients with neuroblastoma.

The differentiation status of T cells present in the starting product emerges as an important parameter for generating CAR-T cell products capable of proliferation and persistence following adoptive T cell therapy [32,33]. T cells used for adoptive therapy must retain their intrinsic capacity for self-renewal and proliferation to eradicate large, established tumors. Preclinical xenograft models have shown that CAR-T cells derived from $CD8^+$ and $CD4^+$ T_N and T_{CM} subsets are more potent than those manufactured from T_{EM} subsets, and that a combination of the optimal $CD8^+$ and $CD4^+$ T cell subsets leads to synergistic antitumor activity [27]. We demonstrated that cryopreserved G-CSF-stimulated apheresis products contain sufficient numbers of CD4 and CD8 T cell precursors with T naïve and central memory differentiation subsets with replicating potential and the capacity to generate large numbers of effector T cells after tumor stimulation. A comparison of the T cell phenotype from the cryopreserved G-CSF-stimulated PBSCs with the T cell phenotype from the PBSCs of the first 5 patients enrolled in ENCIT-01, in whom the CAR-T cells were generated from freshly harvested apheresis products [6], revealed that the CD8 repertoire of the G-CSF-stimulated apheresis products contained higher frequencies of naïve and central memory T cells, indicating (1) greater ex vivo expansion capability, (2) ability to give rise to memory and effector T cell subsets, (3) enhanced in vivo persistence, and (4) improved antitumor activity [34,35].

Based on our findings, we conclude that biobanked PBSCs collected by apheresis offer an excellent alternative source for CAR-T cell manufacturing. Future detailed phenotypic and ex vivo expansion analyses of starting materials, as well as preselection of defined functional T cell subsets and functional analysis of the final CAR-T cell products administered to patients will be essential to develop the most effective CAR-T cell products.

ACKNOWLEDGMENTS

The authors thank Kathy Astrahantseff for proofreading the manuscript.

Financial disclosure: A.K. was supported by the German Research Foundation and is a participant in the BIH-Charité Clinical Scientist Program funded by the Charité University Hospital and the Berlin Institute of Health. M.C.J. was supported by an SU2C/St. Baldrick’s Pediatric Immunogenomics Dream Team Grant. The Jensen Laboratory at the Ben Towne Center for Childhood Cancer Research is the recipient of financial support from the Ben Towne Pediatric Cancer Research Foundation, Make Some Noise: Cure Kids Cancer Foundation Incorporation, Seattle Children’s Guild Association, Andrew McDonough B+ Foundation, Journey 4 A Cure, Zulily, St. Baldrick’s Foundation, and Life Sciences Discovery Fund.

Conflict of interest statement: M.C.J. is a founder and equity holder of Juno Therapeutics, Inc. There are no conflicts of interest to report.

SUPPLEMENTARY MATERIALS

Supplementary material associated with this article can be found, in the online version, at doi:10.1016/j.bbmt.2018.10.004.

REFERENCES

1. Maris JM, Hogarty MD, Bagatell R, Cohn SL. Neuroblastoma. *Lancet*.. 2007;369:2106–2120.
2. Hero B, Kremens B, Klingebiel T, et al. Does megatherapy contribute to survival in metastatic neuroblastoma? A retrospective analysis. German Cooperative Neuroblastoma Study Group. *Klin Padiatr*.. 1997;209:196–200.
3. Matthay KK, DeSantes K, Hasegawa B, et al. Phase I dose escalation of 131I-metaiodobenzylguanidine with autologous bone marrow support in refractory neuroblastoma. *J Clin Oncol*.. 1998;16:229–236.
4. London WB, Castel V, Monclair T, et al. Clinical and biologic features predictive of survival after relapse of neuroblastoma: a report from the International Neuroblastoma Risk Group project. *J Clin Oncol*.. 2011;29:3286–3292.
5. Künkele A, Johnson AJ, Rolczynski LS, et al. Functional tuning of CARs reveals signaling threshold above which CD8+ CTL antitumor potency is attenuated due to cell Fas-FasL-dependent AICD. *Cancer Immunol Res*.. 2015;3:368–379.
6. Künkele A, Taraseviciute A, Finn LS, et al. Preclinical assessment of CD171-directed CAR T-cell adoptive therapy for childhood neuroblastoma: CE7 epitope target safety and product manufacturing feasibility. *Clin Cancer Res*.. 2017;23:466–477.

7. Allory Y, Matsuoka Y, Bazille C, Christensen EI, Ronco P, Debiec H. The L1 cell adhesion molecule is induced in renal cancer cells and correlates with metastasis in clear cell carcinomas. *Clin Cancer Res.*. 2005;11: 1190–1197.
8. Fogel M, Gutwein P, Mechtersheimer S, et al. L1 expression as a predictor of progression and survival in patients with uterine and ovarian carcinomas. *Lancet.*. 2003;362:869–875.
9. Raveh S, Gavert N, Ben-Ze'ev A. L1 cell adhesion molecule (L1CAM) in invasive tumors. *Cancer Lett.*. 2009;282:137–145.
10. Matthay KK, Villablanca JG, Seeger RC, et al. Treatment of high-risk neuroblastoma with intensive chemotherapy, radiotherapy, autologous bone marrow transplantation, and 13-cis-retinoic acid. Children's Cancer Group. *N Engl J Med.*. 1999;341:1165–1173.
11. Singh N, Perazzelli J, Grupp SA, Barrett DM. Early memory phenotypes drive T cell proliferation in patients with pediatric malignancies. *Sci Transl Med.*. 2016;8. 320ra323.
12. Porter DL, Hwang WT, Frey NV, et al. Chimeric antigen receptor T cells persist and induce sustained remissions in relapsed refractory chronic lymphocytic leukemia. *Sci Transl Med.*. 2015;7. 303ra139.
13. Ceppi F, Rivers J, Annesley C, et al. Lymphocyte apheresis for chimeric antigen receptor T-cell manufacturing in children and young adults with leukemia and neuroblastoma. *Transfusion.*. 2018;58:1414–1420.
14. Beloki L, Ramirez N, Olavarria E, Samuel ER, Lowdell MW. Manufacturing of highly functional and specific T cells for adoptive immunotherapy against virus from granulocyte colony-stimulating factor-mobilized donors. *Cytotherapy.*. 2014;16:1390–1408.
15. Samuel ER, Beloki L, Newton K, Mackinnon S, Lowdell MW. Isolation of highly suppressive $CD25^{+}FoxP3^{+}$ T regulatory cells from G-CSF-mobilized donors with retention of cytotoxic anti-viral CTLs: application for multifunctional immunotherapy post stem cell transplantation. *PLoS One.*. 2014;9:e85911.
16. Clancy LE, Blyth E, Simms RM, et al. Cytomegalovirus-specific cytotoxic T lymphocytes can be efficiently expanded from granulocyte colony-stimulating factor-mobilized hemopoietic progenitor cell products ex vivo and safely transferred to stem cell transplantation recipients to facilitate immune reconstitution. *Biol Blood Marrow Transplant*. 2013;19: 725–734.
17. Rossetti M, Gregori S, Roncarolo MG. Granulocyte-colony stimulating factor drives the in vitro differentiation of human dendritic cells that induce anergy in naive T cells. *Eur J Immunol.*. 2010;40:3097–3106.
18. Wang X, Chang WC, Wong CW, et al. A transgene-encoded cell surface polypeptide for selection, in vivo tracking, and ablation of engineered cells. *Blood.*. 2011;118:1255–1263.
19. Gonzalez S, Naranjo A, Serrano LM, Chang WC, Wright CL, Jensen MC. Genetic engineering of cytolytic T lymphocytes for adoptive T-cell therapy of neuroblastoma. *J Gene Med.*. 2004;6:704–711.
20. Kreissman SG, Seeger RC, Matthay KK, et al. Purged versus non-purged peripheral blood stem-cell transplantation for high-risk neuroblastoma (COG A3973): a randomised phase 3 trial. *Lancet Oncol.*. 2013;14: 999–1008.
21. Park JR, Scott JR, Stewart CF, et al. Pilot induction regimen incorporating pharmacokinetically guided topotecan for treatment of newly diagnosed high-risk neuroblastoma: a Children's Oncology Group study. *J Clin Oncol.*. 2011;29:4351–4357.
22. Ellestad KK, Lin J, Boon L, Anderson CC. PD-1 controls tonic signaling and lymphopenia-induced proliferation of T lymphocytes. *Front Immunol.*. 2017;8:1289.
23. Slaney CY, Toker A, La Flamme A, Backström BT, Harper JL. Naive blood monocytes suppress T-cell function: a possible mechanism for protection from autoimmunity. *Immunol Cell Biol.*. 2011;89:7–13.
24. Martinez FO, Sica A, Mantovani A, Locati M. Macrophage activation and polarization. *Front Biosci.*. 2008;13:453–461.
25. Yang S, Gattinoni L, Liu F, et al. In vitro generated anti-tumor T lymphocytes exhibit distinct subsets mimicking in vivo antigen- experienced cells. *Cancer Immunol Immunother.*. 2011;60:739–749.
26. Simon S, Vignard V, Florenceau L, et al. PD-1 expression conditions T cell avidity within an antigen-specific repertoire. *Oncoimmunology*. 2015;5 e1104448.
27. Sommermeyer D, Hudecek M, Kosasih PL, et al. Chimeric antigen receptor-modified T cells derived from defined $CD8^{+}$ and $CD4^{+}$ subsets confer superior antitumor reactivity in vivo. *Leukemia.*. 2016;30:492–500.
28. Berger C, Jensen MC, Lansdorp PM, Gough M, Elliott C, Riddell SR. Adoptive transfer of effector $CD8^{+}$ T cells derived from central memory cells establishes persistent T cell memory in primates. *J Clin Invest.*. 2008;118:294–305.
29. Klebanoff CA, Gattinoni L, Torabi-Parizi P, et al. Central memory self/tumor-reactive $CD8^{+}$ T cells confer superior antitumor immunity compared with effector memory T cells. *Proc Natl Acad Sci U S A*. 2005;102: 9571–9576.
30. Bryn T, Yaqub S, Mahic M, Henjum K, Aandahl EM, Taskén K. LPS-activated monocytes suppress T-cell immune responses and induce $FOXP3^{+}$ T cells through a COX-2-PGE2-dependent mechanism. *Int Immunol.*. 2008;20: 235–245.
31. Gu BJ, Sun C, Fuller S, Skarratt KK, Petrou S, Wiley JS. A quantitative method for measuring innate phagocytosis by human monocytes using real-time flow cytometry. *Cytometry A*. 2014;85:313–321.
32. Busch DH, Frässle SP, Sommermeyer D, Buchholz VR, Riddell SR. Role of memory T cell subsets for adoptive immunotherapy. *Semin Immunol.*. 2016;28:28–34.
33. Jensen MC, Riddell SR. Design and implementation of adoptive therapy with chimeric antigen receptor-modified T cells. *Immunol Rev.*. 2014;257: 127–144.
34. Restifo NP, Gattinoni L. Lineage relationship of effector and memory T cells. *Curr Opin Immunol.*. 2013;25:556–563.
35. Kalos M, Levine BL, Porter DL, et al. T cells with chimeric antigen receptors have potent antitumor effects and can establish memory in patients with advanced leukemia. *Sci Transl Med.*. 2011;3. 95ra73.